Response of Profiled High-Density Polyethylene Pipe in Hoop Compression

IAN D. MOORE AND FUPING HU

Profiled polymer pipe is a three-dimensional structural form that behaves in a three-dimensional manner when subjected to soil pressures during burial. The three-dimensional response of profiled high-density polyethylene (HDPE) pipe was recently measured in a soil cell at the University of Massachusetts. The profile tested featured a corrugated section fitted with a smooth internal liner. A finite element analysis for determining the response of buried profiled pipe has been developed by the first author. The soil cell results are examined using the three-dimensional finite element analysis. Distributions of circumferential and axial stress and strain are considered in the profiled pipe and in the soil surrounding it, and different responses of the corrugation and the liner are examined. The analysis is used to examine performance limits for profiled HDPE pipe under large hoop compressions.

To successfully engineer buried profiled high-density polyethylene (HDPE) pipe, several aspects of the soil-structure system should be considered. Some of these issues are common to both HDPE and other pipe products, but others are unique to the HDPE pipes, which are the primary focus of this study. Understanding these issues is necessary to design efficient, reliable products suitable for use in a wide range of applications.

Initially, the structural design of buried HDPE pipe was based on semi-empirical procedures developed for flexible metal pipe products [in particular, the Iowa equation developed by Spangler (*1*)]. Pipe design has generally focused on the change in diameter across the pipe section, although levels of circumferential hoop and bending stress, circumferential strain, and the possibility of circumferential buckling have also been considered.

Culvert and buried pipe technology was significantly advanced in the 1960s and 1970s after the development of closed form solutions [Burns and Richard (*2*)] and finite element analyses [Katona (*3*)] of pipe-soil interaction. These studies have contributed much to the understanding of buried pipe response at working loads. In particular, the behavior of buried profiled polyethylene pipe has been examined using two-dimensional finite element analyses [Chua (*4*) and Katona (*5*)] and three-dimensional finite element analysis [Moore (*6*)]. These computational tools have the potential to ensure that the structural design of buried HDPE pipe is based on rigorous engineering principles, and that it is both safe and efficient.

Concerns remain about several specific issues for HDPE pipes. The three-dimensional nature of the corrugated pipe profile has prompted interest in distribution of circumferential and axial stresses in the profile and the contribution of the liner to the overall structural performance. The time-dependent nature of polyethylene response has led to a series of questions about effective modulus, pipe stiffness, stress relaxation, and creep. Furthermore, the move toward limit state design in North America is prompting demands for more information about stability and serviceability limits for HDPE pipe.

A pipe buried deeply within an earth embankment is subjected to vertical and horizontal field stresses as a result of the overburden and the lateral earth pressures. Those earth pressures lead to the development of hoop compressions in the pipe, which can cause important circumferential strains.

Responding to the demand for direct measurement of pipe performance under hoop compression, a test cell was developed recently by Selig at the University of Massachusetts (UMass) (*7*). This report describes the results of a theoretical investigation of those tests, examining the development over time of circumferential stress and strain and the three-dimensional response of the corrugation and internal lining of the pipe. The analysis is used to consider performance limits for pipe subjected to large hoop compressions.

UMASS COMPRESSION CELL TESTS

Three tests were performed in the compression cell at UMass and involved the application of uniform radial compressions to the external boundary of a thin ring of soil placed around the pipe. Pipe deformations at various stress levels were monitored over time. Details of the test equipment and procedure are described by Selig et al. (*7*) and DiFrancesco (*8*).

Selig et al. (*7*) have clearly stated that the uniform soil support and axisymmetric stress condition the cell induces around the pipe is not wholly representative of the pipe condition in the field. However, the cell provides valuable test data under controlled stress conditions. It induces substantial compressions up to and beyond those that develop in the field [Hashash and Selig (*9*)]. Furthermore, the measurements of pipe response can be used to calibrate a theoretical analysis that can then be used to estimate pipe response under more realistic stress conditions.

One pipe composed of each of three materials was tested. The first material represents a current production compound. The other two are nonproduction compounds.

1. Virgin polyethylene (cell classification 32430C);
2. Recycled material (50 percent virgin material, 50 percent reground industrial material); and
3. Virgin material, together with 7 percent $CaCO_3$.

All three materials were stabilized with 2 percent carbon black (they will be referred to as the "virgin," "recycled," and "filled" materials).

Geotechnical Research Centre, Faculty of Engineering Science, The University of Western Ontario, London, Ontario, N6A 5B9, Canada.

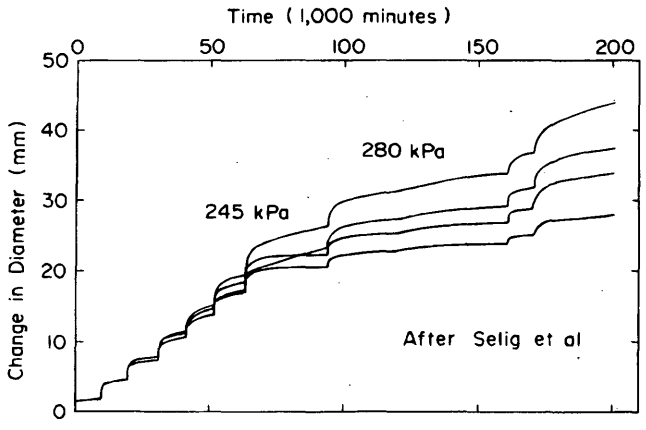

FIGURE 1 Diameter change with time recorded during the compression cell test on a pipe segment composed of the filled material (*7*).

The work at UMass showed that the tensile properties for all three materials were similar, as were the properties measured from samples cut from the pipe in the circumferential and axial directions [Kakulavar (*10*)]. Tests were inconclusive regarding the differences between compressive and tensile properties.

Figure 1 shows one trace of diameter change versus time for the pipe composed of $CaCO_3$-filled resin. This test featured the highest level of applied radial stress. It was loaded in 10 stress increments of 35 kPa (5 psi). The first six radial stress increments were held for about 10,000 min. The seventh to tenth stress increments were held for 30,000, 65,000, 10,000, and 30,000 min, respectively.

Pipe deflection measurements are shown at four different locations. The deflections are reasonably uniform during the first four increments. Beyond that, differences between minimum and maximum measured deflection are 10, 17, and 25 percent, growing steadily up to 45 percent at the end of the test.

Load deflection response for the pipe composed of filled material is shown in Figure 2. Pipe deflection at the end of each deflection increment is shown relative to the applied pressure. The test cell successfully loaded the pipe well beyond current use of the product in the field. Figure 2 shows the points at which the internal liner of the pipe was observed to develop "ripples" and to start cracking. These observed responses have been proposed as potential performance limits for these structures [Selig et al. (*7*)].

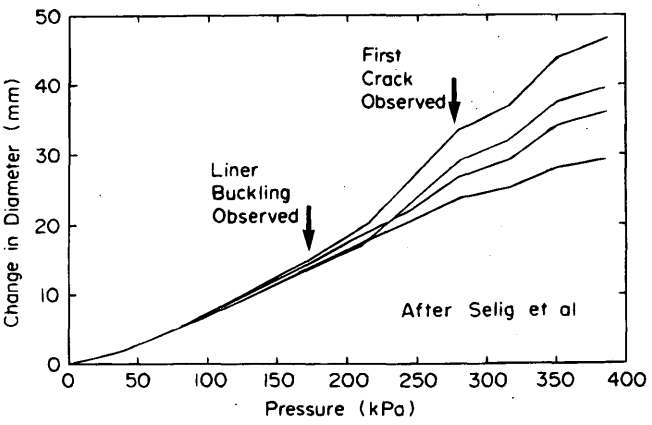

FIGURE 2 Load deflection response recorded during the compression cell test on a pipe segment composed of the filled material (*7*).

FINITE ELEMENT MODELING

Since much of this study focuses on the analysis and interpretation of observed pipe behavior, it is important to briefly describe the computer analysis used. For corrugated pipes with annular (not helical or spiral) design and with linear elastic or viscoelastic material response, the axisymmetric geometry can be used to simplify the analysis [Moore (*6*)]. A two-dimensional finite element mesh is used to model the geometry and strain fields in the r, z plane (Figure 3), and a Fourier series is used to model variations around the pipe circumference. Pipe response to each Fourier harmonic around the pipe is determined independently, and the full pipe response is assembled from each of these separate components using superposition.

To determine the pipe response in the compression cell of Selig et al. (*7*), only one axisymmetric loading harmonic is required (Figure 4).

One specific lined corrugated pipe profile has been examined by Selig et al. (*7*), and a finite element mesh has been developed for analysis of that profile. Figure 5 shows the mesh used to analyze the pipe in the compression cell. The analysis features explicit modeling of the three-dimensional pipe profile, as well as the thin ring of soil that is placed between the pipe and the PVC bladder around the outside. More than 800 six-noded triangular finite elements were used, 184 for one-half corrugation of the annular pipe and 661 for the granular soil surrounding it. Smooth rigid boundaries are used at the edges of the half corrugation, since these are lines of symmetry of the long axially constrained pipe sample. The pipe and soil are modeled as "bonded" together. A uniform radial compression is applied at the external boundary, simulating the pressures imposed by the PVC bladder used in the UMass compression cell.

HDPE exhibits very noticeable time-dependent behavior, and any detailed evaluation of HDPE pipe response will certainly involve a treatment of this constitutive characteristic. Fortunately,

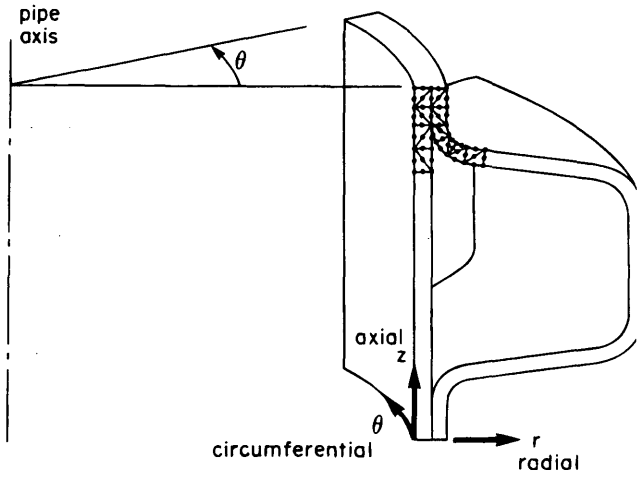

FIGURE 3 Finite element model for three-dimensional profiled pipe analysis.

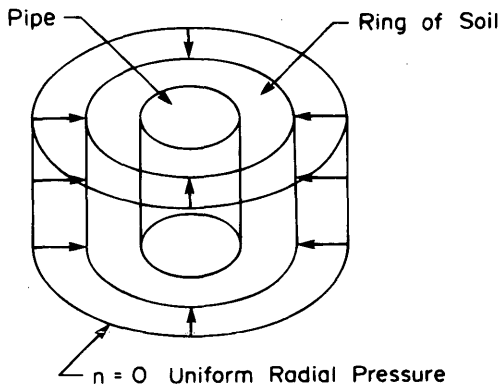

FIGURE 4 Loading and harmonic model used for the hoop compression test.

polyethylene appears to respond in a linear viscoelastic manner at stress levels up to about 30 to 50 percent of tensile yield stress. Well-established techniques in applied mechanics can be used for modeling such behavior. In particular, conventional rheology using sets of "springs" and "dashpots" is used. The multi-Kelvin model has been implemented featuring one independent spring and a series of nine Kelvin elements (each a spring and dashpot in parallel). For linear behavior of both structures, Laplace transforms are used to convert the linear viscoelastic problem into an equivalent elastic problem. Analysis is performed in the "Laplace" domain, and the real displacements, strains, and stresses are found after inversion of the Laplace transforms (*11*). For problems featuring nonlinear soil behavior, an iterative analysis is undertaken directly in the time domain, using the procedure of Zienkiewicz et al. (*12*) for the linear viscoelastic material (the pipe), and an incremental elastic-plastic analysis for the soil [Zienkiewicz (*13*)].

Material parameters for the polyethylene used in pipe manufacture have been developed by Moore and Hu (*14*) based on the data of Janson (*15*), Chua (*4*), and Hashash (*16*). The independent spring has a modulus of 1120 MPa (161.2 ksi), and moduli for the Kelvin springs are 3615.6 MPa (520.2 ksi), 0.845×3615.6 MPa, $0.845^2 \times 3615.6$ MPa, . . . , $0.845^8 \times 3615.6$ MPa, and Kelvin dashpot viscosities are 0.503 MPa.days (72.4 psi.days), 5.03 MPa.days, up to 5.03×10^7 MPa.days.

More difficult is the choice of soil parameters. The soil is characterized as either an isotropic linear elastic or elastic-plastic material. Elastic soil models have been found to be a reasonable first approximation to many buried pipe problems [Burns and Richard (*2*), Katona (*3*), and Moore and Brachman (*17*)]. It requires the selection of elastic modulus and Poisson's ratio. When granular soil is subjected to low confining stresses, soil failure can occur followed by an elastic-plastic response. Both soil models have been used to evaluate the development of plastic deformations in the soil and to examine their significance.

A valuable reference for soil properties is the laboratory study reported by Selig (*18*). A series of different partially saturated soils were examined, with stress strain characteristics measured at a number of different relative densities.

DiFrancesco (*8*) describes the backfill as a moist coarse-to-fine sand, and denotes a poorly graded material under the Unified Classification System. He suggests that at the measured water content of 3.5 percent, unit weight for the compactive effort used to backfill the compression cell is 113 kN/m^3. This is 92 percent of the maximum dry unit weight for the Proctor test, and 96 percent of the Proctor dry unit weight at a water content of 3.5 percent.

Selig (*18*) does not provide data for poorly graded materials, and the actual unit weight or relative density was not measured after the soil was placed around the pipe and pressurised in the compression cell.

To resolve these problems, an iterative approach was used to estimate the soil properties. First, Poisson's ratio was estimated as 0.3, which is reasonable for a granular soil at low levels of strain. Next, a series of calculations were performed to evaluate pipe deflections at 1,000 min, based on soil modulus for well-graded sands at a variety of relative densities. Using the Lagrangian method to interpolate between densities, a match between predicted and measured deflections was obtained for an SW93 material. Elastic modulus is 40 MPa (5.8 ksi) at that stress level.

This relative density appears to be reasonable given the 92 to 96 percent range quoted previously and assuming the SP material performs as Selig's SW material. This good performance for an SP material may be because the soil is not simply a single grain-size material (it has a uniformity coefficient C_U of 3.6 and a coefficient of curvature C_z of 1.3; the former is not that far from the 4 and 6 minimums required for well-graded gravels and sands; the latter value is within the 1 to 3 range characteristic of well-graded soils).

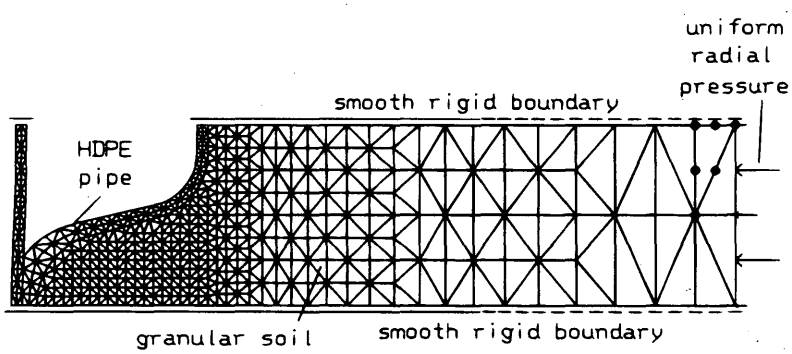

FIGURE 5 Finite element mesh used for analysis of the compression cell tests (*7*).

Several calculations were performed using these soil properties to examine the response of the pipe in the soil cell.

INVESTIGATION OF SOIL RESPONSE

The soil model used treats the soil as a uniform isotropic elastic continuum. Before proceeding with the investigation of the pipe, it is useful to examine the nature of stresses in the soil and review the differences between elastic and elastic-plastic soil models.

The shear stresses in real soil materials are limited by the shear strength. If shear stress estimated using elastic analysis is in excess of the shear strength, then it is likely that the soil would not remain elastic. For a dry granular soil, the soil strength is usually expressed using an angle of internal friction, ϕ. That angle controls the maximum normal stress in the soil (the major principal stress σ_1), which is limited by the magnitude of the minimum normal stress (the minor principal stress σ_3):

$$\sigma_1 \leq \sigma_3 \tan^2(45 + \phi/2) \quad (1)$$

or

$$\frac{\sigma_1}{\sigma_3} \leq \tan^2(45 + \phi/2) \quad (2)$$

Figure 6 shows contours of principal stress ratio σ_1/σ_3. By comparing stress ratio σ_1/σ_3 to values of $\tan^2(45 + \phi/2)$, it is possible to gauge the extent of shear failure in the soil. When stress ratio estimates from the elastic analysis exceed $\tan^2(45 + \phi/2)$, shear failure is expected.

Table 1 gives a number of $\tan^2(45 + \phi/2)$ values for soil materials. An examination of Figure 6 (in addition to Table 1) shows that zones of shear failure are likely to occur near the pipe. For the soil placement used in the UMass compression cell tests, the relative density estimate of 93 percent implies a friction angle ranging from 42° to 48°. According to Figure 6 and Table 1, the zone of soil in the corrugation valley and a small zone at the corrugation crest should experience shear failure (the soil in the corrugation valley is expected to have lower density, strength and stiffness in any case caused by the difficulties of compacting soil in this region).

These calculations imply that the use of an elastic soil model may not be appropriate.

To check that elastic analysis provides a reasonable prediction of the extent of soil failure, a nonlinear analysis has been performed using the elastic-plastic soil model. This analysis provided a yield zone for the SW93 soil, which closely matches the location based on a stress ratio of 5.8 ($\phi = 45°$). Comparisons of deflection, stress, and strain revealed that the yield in the soil and the subsequent nonlinear soil response does little to change the pipe stresses and displacement. For simplicity, therefore, the results quoted in this study are for elastic soil response.

LOCAL STRESS DISTRIBUTIONS

Calculations of stress distribution within the pipe profile have been made for a radial stress of 35 kPa (5 psi) applied by the air bladder at the outside of the soil ring. The circumferential (hoop) stress σ_θ and axial (longitudinal) stress σ_z are examined, as defined in Figure 7. These stresses are distributed in some manner across the profile. The manner in which they generate local bending moments m_θ and m_z locally in the corrugation and liner elements of the profile can also be inferred.

Figure 8 shows contours of circumferential stress. It reveals that three-dimensional effects occur in the profile, particularly in the pipe liner. A fully compressive stress field develops in the profile in the hoop direction. Compressions (shown as negative quantities in Figure 8) develop in the circumferential direction, ranging in magnitude from 0.5 MPa to 0.6 MPa (70 psi to 85 psi) throughout most of the corrugation. In the liner, local bending causes compressions to drop below 0.1 MPa (10 psi) at the outside of the liner (*i.e.*, at the surface not in contact with the fluid carried in the pipe). This occurs midspan (*i.e.*, at the centerline of the liner section that stretches from one corrugation valley to the other). Hoop compressions also drop below 0.4 MPa (60 psi) on the inside of the liner where the liner connects to the corrugation. Hoop compressions increase to a maximum of more than 0.8 MPa (100 psi) at the outside of the liner at the liner-corrugation connection.

An almost uniform compressive hoop stress of the type seen in Figure 8 for the corrugation can be predicted using two-dimensional analysis. Such compressions are generally not of great concern, and although high compressions may cause yield (as defined by an offset yield stress), they should not lead to rupture and are unlikely to cause distress in the polyethylene material. The effect of the three-dimensional profile on the hoop stress distribution can be summarized as local bending in the liner, causing variations in stress above and below the uniform hoop compression.

Figure 9 shows contours of axial stress. It also indicates that three-dimensional effects occur in the pipe liner. Compressive (negative) stresses in the liner are similar in magnitude to those in the hoop direction (the lowest contour interval shown corresponds to −0.6 MPa or −90 psi, the lowest axial compression is less than −0.8 MPa or 110 psi). In the corrugation, the stress field is generally compressive, ranging in magnitude from 0 to −0.2 MPa (30

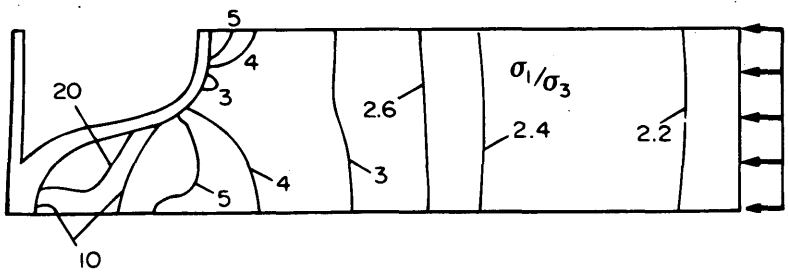

FIGURE 6 Stress ratio calculated for an elastic soil material; pipe response in the compression cell with 35 kPa (5 psi) bladder pressure; stresses at 1,000 min.

TABLE 1 Stress Ratio as Function of Friction Angle and Relative Density

σ_1/σ_3	ϕ	soil
3	30°	SW62
4	37°	SW80
5	42°	SW90
10	55°	SW98

psi). The latter value corresponds to a small region of local bending at the crest of the corrugation.

Tensile (positive) axial stresses occur at certain points in the corrugation and the liner. In the liner, tensions occur on the inside surface, adjacent to the liner corrugation junction. Careful examination of the local stresses shows a peak tension of 0.84 MPa or 120 psi (the maximum contour shown is 0.4 MPa, 60 psi). Tension also develops on the outside of the liner midspan. The value at this location is about 0.4 MPa (60 psi).

To help explain the nature of the local bending, Figure 10 shows the finite element prediction of deformed shape after 1,000 min at 35 kPa (5 psi) radial pressure. Careful examination of the deformed and underformed geometry of the profile reveals that the local bending stresses shown in Figure 9 are associated with a nonuniform radial movement that occurs along the liner. For the corrugation, continuous contact with the soil around the pipe leads to an almost uniform radial contraction (compression of the pipe with movement toward the pipe axis). For the liner, however, only that section bonded to the corrugation moves inwardly to that extent. The remainder of the liner (that section spanning from across one corrugation valley to the other) resists that radial movement, and at midspan less than half the radial movement experienced by the corrugation occurs. The liner, therefore, is acting like an encastered beam, where rotations at midspan and at the liner-corrugation junction are prevented, and the liner corrugation junction moves relative to the liner midpoint. Axial bending stresses, therefore, develop in the liner (in the direction of the beam axis), consisting of the regions of compression and tension shown in Figure 9.

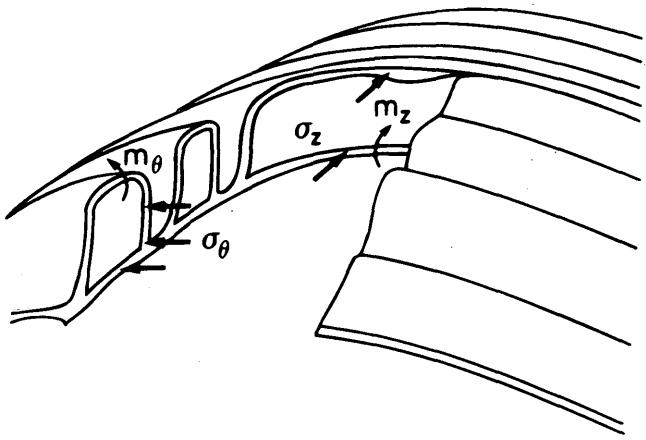

FIGURE 7 Schematic showing circumferential stress σ_θ and axial stress σ_z acting in the HDPE pipe profile.

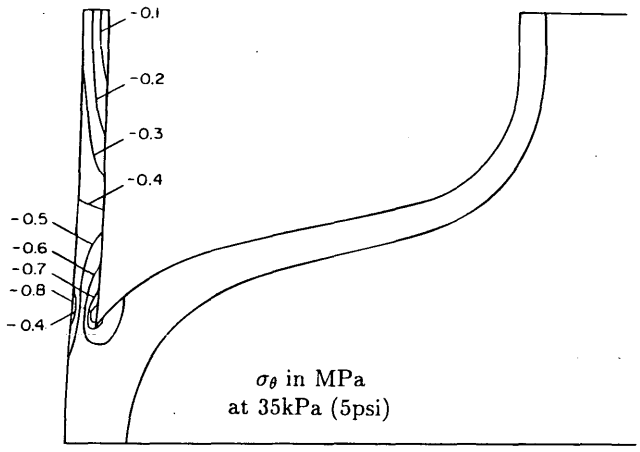

FIGURE 8 Contours of circumferential stress σ_θ acting in the HDPE pipe profile with 35 kPa (5 psi) bladder pressure in the UMass compression cell; stresses at 1,000 min.

LINER RIPPLING

Selig et al. (*7*) report that when each of the pipes tested in the UMass compression cell were loaded sufficiently to cause about 1.9 percent radial contraction, a series of regularly spaced ripples were observed in the liner. Figure 11 is a schematic of the phenomenon. A series of ripples developed around the pipe circumference, as well as along the pipe axis. As effective burial depth was increased, virtually the whole of the liner of the pipe specimens being tested developed these regular, uniformly sized wave-like deformations.

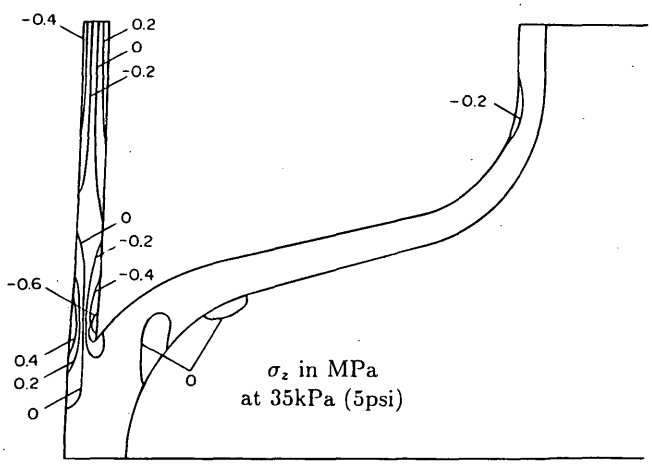

FIGURE 9 Contours of axial stress σ_z acting in the HDPE pipe profile with 35 kPa (5 psi) bladder pressure in the UMass compression cell; stresses at 1,000 min.

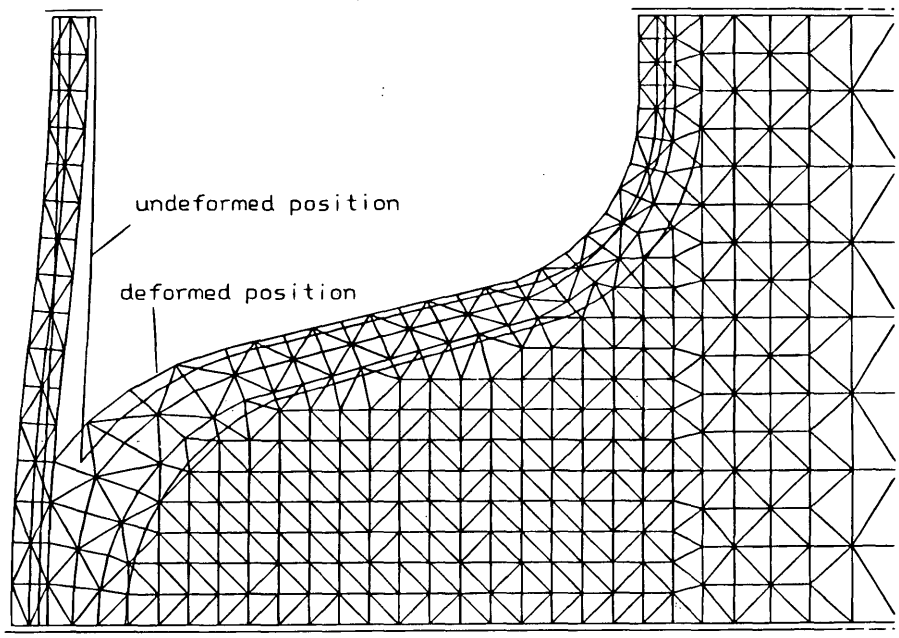

FIGURE 10 Deformations of profile at 35 kPa (5 psi) bladder pressure in the UMass compression cell; prediction for 1,000 min.

One possibility is that these ripples are local buckles that develop from compressive stresses that occur in the hoop direction as the pipe contracts into the cavity. This type of local buckling develops in many stiffened shell or plate structures (such as aircraft wings), and is well known for being a stable phenomenon (the load capacity of the structural element does not decrease after it has buckled). Such stable plate and shell buckling mechanisms are amenable to linear buckling analysis (an analysis developed on the basis of the original undeformed structural geometry).

To investigate whether the ripples were the result of local shell buckling, a linear three-dimensional buckling solution of thin cylindrical shells was used to determine the radial contraction necessary to cause buckling (*19*). The valley of the corrugation was assumed to be sufficiently thick to prevent rotation of the liner at the corrugation-liner junction, so the wavelength of the buckles in the longitudinal direction was assumed equal to the "clear span" of the liner from one corrugation valley to the next. The liner was also assumed to be a flat, uniform thickness cylindrical shell.

For a cylindrical shell of radius 307 mm (12.1 in.), thickness of 2.8 mm (0.11 in.), and "clear span" of 77 mm (3.03 in.), the analysis indicates that elastic buckling occurs at a radial contraction of 1.8 percent, and with 40 buckles developing around the pipe circumference. Selig et al. (*7*) report that rippling was first observed at a radial contraction of 1.9 percent, and observed about 50 ripples around the circumference of the pipe.

It appears, therefore, that the ripples observed in the pipe tests are the result of local buckling in the pipe liner.

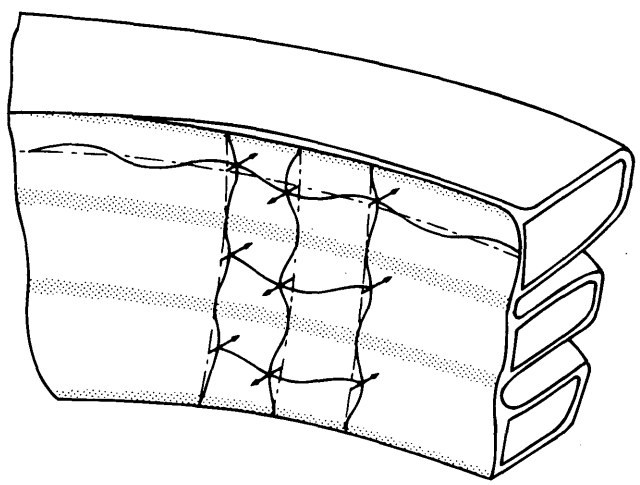

FIGURE 11 Schematic of the rippling deformations observed at 1.9 percent radial contraction (*7*).

LOCAL TEARS IN LINER AT HIGH HOOP COMPRESSION

Selig et al. (*7*) report that one of the pipes tested in the UMass compression cell, which was loaded to very high cell pressure, developed a regular series of short circumferential tears in the liner close to the liner-corrugation junction.

The contours of axial stress shown in Figure 9 indicate that the local tearing is located directly at the point of highest tension. Clearly, these tensions in the axial direction may be wholly or partly responsible for the tears that occur normal to them in the circumferential direction. The possibility exists that the tears are a ductile rupture caused by excessive local bending stress associated with the nonuniform liner contraction.

Selig et al. (*7*) report that the small, regularly spaced tears were observed through the liner at about 270 kPa (39 psi) cell pressure (equivalent to 30 m or more of pipe burial). This is about 7.7 times the pressure acting to generate the axial stresses shown in Figure 8.

Simple scaling of those stress values suggests that local tension of approximately 6 MPa (900 psi) is expected at this load level. This is close to the long-term AASHTO yield stress.

The value of local axial bending stress is approximate. Shear failure in the soil placed in the corrugation valley is expected to increase local bending stress, whereas the stiffening of the soil material expected with increasing applied stress would act to decrease the local stresses in the polyethylene. Some stress relaxation is also expected, which would decrease stresses.

Axial stresses will also be modified by the local buckles that develop in the liner. These local buckles will increase the axial tensions at the inner surface where the buckle moves away from the pipe axis, and will decrease the axial tension where the buckle moves toward the pipe axis. The short, regularly spaced tears observed in the pipe tests match the positions where maximum tension is expected.

To obtain further information concerning the tears observed during the compression tests, an electron micrograph was taken of the polyethylene rupture surface revealing a rupture surface consistent with ductile tearing (Sheasby, J. S., personal communication (1994)).

It appears then that the regular pattern of tears in the liner represent a ductile failure resulting from the local axial tensions (Figure 9) as well as some additional tension associated with the local buckling.

PERFORMANCE LIMITS

The local buckling and local tearing phenomena outlined in the report relate to the three-dimensional effects in lined corrugated HDPE pipe and have implications for pipe design.

Local buckling in the liner does not cause overall instability of the lined corrugated pipe because the corrugation continues to provide structural support. This form of deformation may, however, be treated as a serviceability limit caused by some effect on the hydraulic performance of the sewer pipe.

The axial tensions in a lined corrugated pipe should be examined during the design of highly loaded lined corrugated pipe. The corrugation integrity does not appear to be threatened, and the pipes tested in the compression cell did not experience instability. However, the development of local tears in the pipe lining is obviously undesirable. A parametric study estimating axial stresses for pipes in situ would assist in the design of these pipes for very deep burial. Future research to examine other profiled HDPE pipe products for three-dimensional effects would also be valuable.

CONCLUSIONS

The three-dimensional response of a lined corrugated HDPE pipe was observed during the testing program undertaken at the University of Massachusetts. Analysis of the pipe-soil system in the compression test cell has revealed that local bending occurs in the pipe liner, modifying the stress state in the pipe beyond that predicted using conventional two-dimensional pipe-soil interaction analysis. The local bending is confined to the liner, and it is likely that a corrugated unlined pipe will not be subject to the same phenomenon.

Conventional "ring" theory predictions for profiled pipe response cannot estimate levels of axial stress, but the three-dimensional analysis has clearly shown that axial bending stresses do develop at certain locations in the pipe profile. The junction between the liner and the corrugation is the site of the largest axial tensions. These axial tensions develop on the inside surface of the liner and exceed the circumferential tensions that develop. The magnitude of these local axial stresses suggests that the liner tearing observed by Selig et al. (*17*) is associated with ductile tensile failure at these locations.

Three-dimensional linear buckling analysis reveals that the rippling deformations observed by Selig et al. (*7*) are, in fact, local buckles that are a stable buckling mechanism often found in stiffened plate or shell structures.

ACKNOWLEDGMENTS

This work was sponsored by the Corrugated Plastic Pipe Association and the Natural Sciences and Engineering Research Council of Canada through an industrially oriented research grant. Theoretical models were developed with the assistance of research and equipment grants from the Natural Sciences and Engineering Research Council of Canada. Assistance was also provided by E. T. Selig, who supplied details of the hoop compression tests.

REFERENCES

1. Spangler, M. G. Stresses in Pressure Pipelines and Protective Casting Pipes. *Journal of Structural Engineering,* ASCE, Paper 1054, 1956, pp. 33.
2. Burns, J. Q., and R. M. Richard. Attenuation of Stresses for Buried Cylinders. *Proc., Symposium on Soil-Structure Interaction,* ASTM, University of Arizona, 1964, pp. 379–392.
3. Katona, M. G. CANDE: A Modern Approach for the Structural Design and Analysis of Buried Culverts. Report FHWA-RD-77-5. FHWA, Department of Transportation, October 1976.
4. Chua, K. M. *Time-dependent Interaction of Soil and Flexible Pipe.* Ph.D. thesis. A&M University, Texas, 1986.
5. Katona, M. G. Allowable Fill Heights for Corrugated Polyethylene Pipe. *Transportation Research Record,* 1988, pp. 30–38.
6. Moore, I. D. Three Dimensional Time Dependent Models for Buried HDPE Pipe. In *Proc. of the Eighth International Conference on Computer Methods and Advances in Geomechanics* (H. J. Siriwardane, ed.), Morgantown, W.V., A. A. Balkema, Rotterdam, May 1994, pp. 1515–1520.
7. Selig, E. T., L. C. DiFrancesco, and T. J. McGrath. Laboratory Test of Buried Pipe in Hoop Compression. In *Special Technical Publication 1222, Buried Plastic Pipe Technology* (D. Eckstein, ed.), ASTM, Philadelphia, Pa., 1994, pp. 119–132.
8. DiFrancesco, L. C. *Laboratory Testing of High Density Polyethylene Drainage Pipes.* M.Sc. thesis, Department of Civil Engineering, University of Massachusetts, 1993.
9. Hashash, N. M. A., and E. T. Selig. Analysis of the Performance of a Buried High Density Polyethylene Pipe. In *Structural Performance of Flexible Pipes* (G. Mitchell, S. Sargand, and J. Hurd, eds.), Balkema, Rotterdam, 1990, pp. 95–103.
10. Kakulavar, S. *The Effect of Compound Composition on the Mechanical Properties of HDPE Corrugated Pipes.* Master's thesis. Department of Mechanical Engineering, University of Massachusetts, 1993.
11. Moore, I. D. Local Strain in Corrugated Pipe: Experimental Measurements to Test a Numerical Model. *Journal of Testing and Evaluation,* ASTM, March 1994, pp. 132–138.
12. Zienkiewicz, O. C., M. Watson, and I. P. King. A Numerical Method of Visco-elastic Stress Analysis. *Journal of Mechanical Science,* 1968, pp. 807–827.
13. Zienkiewicz, O. C. *The Finite Element Method in Engineering Science.* McGraw-Hill, New York, 1979.

14. Moore, I. D., and E. Hu. Linear Viscoelastic Models for HDPE. *Canadian Journal of Civil Engineering,* (in press), 1995.
15. Janson, L. E. Investigation of the Long Term Creep Modulus for Buried Polyethylene Pipes Subjected to Constant Deflection. In *Advances in Underground Pipeline Engineering* (J. K. Jeyapalan, ed.), Madison, Wis., August 1985, pp. 253–262.
16. Hashash, N. M. A. *Design and Analysis of Deeply Buried Polyethylene Drainage Pipes.* Ph.D. thesis. Department of Civil Engineering, The University of Massachusetts at Amherst, 1991.
17. Moore, I. D., and R. W. Brachman. Three dimensional Analysis of Flexible Circular Culverts. *Journal of Geotechnical Engineering,* ASCE, 1994, pp. 1829–1844.
18. Selig, E. T. Soil Properties for Plastic Pipe Installations. In *Special Technical Publication 1093, Buried Plastic Pipe Technology,* ASTM, Philadelphia, Pa., 1990, pp. 141–158.
19. Moore, I. D. Influence of Rib Stiffeners on the Buckling Strength of Elastically Supported Tubes. *International Journal of Solids and Structures,* 1990, pp. 539–547.

Publication of this paper sponsored by Committee on Subsurface Soil-Structure Interaction.